

A New Method for Predicting Crosstalk of Hand-Assembled Cable Bundles

Chengpan Yang¹, Wei Yan^{1,*}, Yang Zhao¹, Shishan Wang², and Qiangqiang Liu¹

¹ School of Electrical and Automation
Nanjing Normal University, Nanjing, Jiangsu, 210097, China

² Jiangsu Key Laboratory of New Energy Generation and Power Conversion
Nanjing University of Aeronautics and Astronautics, Nanjing, Jiangsu, 210016, China
*61197@njnu.edu.cn

Abstract — Hand-assembled cable bundles are random harness whose crosstalk is difficult to obtain accurately. A crosstalk prediction method of hand-assembled cable bundles is proposed in this paper. The harness is modeled by means of the mean pseudo-random number based on the cascade method. The factors considered in the model include the random exchange of wires position in the wiring harness cross section and the random rotation of the cross section to the ground. A mathematical description of the random exchange of wires position is made by using the row and column transformation of the per unit length RLCG parameter matrix. BP neural network with strong nonlinear mapping ability is introduced to describe the random rotation of wiring harness to the ground. Combined with the finite-difference time-domain (FDTD) method, the crosstalk of the wiring harness is predicted. Experimental results show that the new method has good accuracy in predicting crosstalk of hand-assembled cable bundles. The higher the twisting degree of the wiring harness is, the more concentrated the crosstalk is.

Index Terms — Crosstalk, finite-difference time-domain (FDTD), multiconductor transmission line (MTL), neural network, random bundles.

I. INTRODUCTION

In the field of aerospace and automobile machinery, transmission lines with some similar characteristics will be tightly fixed by manual binding for the convenience of wiring or aesthetics. A large number of transmission lines are laced together, which increases the possibility of electromagnetic interference (EMI) between wires. With the increase of working frequency, the EMI increases significantly, and the crosstalk between wiring harnesses cannot be ignored [1-2].

The traditional transmission line model is a uniform multiconductor transmission line (MTL). The crosstalk value can be obtained by solving the transmission line equation directly [3]. The wire position changes

irregularly along the longitudinal dimension of the hand-assembled cable bundles, and the position of the wires in the section is random and unknown [4-5]. Due to the randomness of the wire position, the per unit length (p.u.l.) RLCG parameter matrix of different spatial locations may be different. It is difficult to predict the crosstalk of hand-assembled cable bundles directly by conventional methods. Broadly speaking, the crosstalk prediction of random wiring harness can be classified into probabilistic model which studies the basic theoretical parameters of crosstalk [6-7], and numerical solution method which simulates the actual random wire trajectories combined with Monte Carlo method [8-10].

In the last two or three decades, a large number of scholars have conducted prediction studies on random wiring harness [11-13], and most scholars have focused their research on the parameter matrix of the harness. In [14], the geometrically symmetrical conventional harness and the irregularly shaped harness are researched. It is verified that the crosstalk between the wires is mainly affected by the position of the generator and the receptor wires. Sun uses the random displacement spline interpolation (RDSI) algorithm to model a random wire harness. The model is used to predict the crosstalk of the harness and evaluate the effectiveness of the method in an experimental environment [15]. In [16-17], the hand-assembled cable bundles are segmented, assuming that the shape of the cross section remains unchanged with the bundle axial direction, and the cross section shape of all the small segments is unchanged. The probability distribution of the inductance and capacitance parameter matrix of a single wire harness cross section is analyzed by using statistical method, and then it is combined with the convolution principle to analyze the “reasonable worst-case” crosstalk of the harness.

The crosstalk of random stranded wiring harness can be predicted by the cascade method [18]. The finite-difference time-domain (FDTD) method is also a special cascade transmission line method in essence. Compared with the conventional cascade method, the FDTD

algorithm has the advantage of more spatial segments, higher accuracy and better adaptability to solve the crosstalk. The FDTD method can solve the crosstalk in time and frequency domain conveniently. Some scholars have applied the FDTD method to solve crosstalk with nonuniform MTLs [19-20].

The above literature only considers the exchange of wires position. Actually, there may be a change in the angle of the cross section to the ground after the wiring harness is segmented. Accordingly, the effect of the angle on the RLCG parameter matrix is explored in this paper. Furthermore, this paper proposes that the exchange of wires position is equivalent to the elementary transformation of the p.u.l. RLCG parameter matrix, which greatly simplifies the analysis of the influence of the random exchange of wires position on crosstalk. Considering the impact of rotation on the harness, the BP neural network is introduced. BP neural network has a strong non-linear mapping ability [21-23].

This paper is organized as follows. A model of the hand-assembled cable bundles is established in Section II. In Section III, the influence of random exchange of wires position on the parameter matrix is firstly expressed mathematically. Then, the influence of cross section rotation on the RLCG parameter matrix is analyzed by the BP neural network. In Section IV, a specific wiring harness model is analyzed by using the new method, probability method, and the experimental method. Section V gives the conclusions of this paper.

II. MODELING OF HAND-ASSEMBLED CABLE BUNDLES

Hand-assembled cable bundles are the random harness, but the “random” of the harness has its own characteristics. Combining the characteristics of the hand-assembled cable bundles model shown in Fig. 1, the n -core harness with length d is evenly divided into N segments, such as the length of S_1 and S_2 is equal. Therefore, the following assumptions are made for the modeling of the random wiring harness:

- 1) The parameters of each wire are identical, including the material and radius of the wire and insulation.
- 2) The transmission line in each segment is regarded as a parallel and uniform transmission line.
- 3) The wires in the harness are close together, and the geometric shapes of the cross sections at different positions remain unchanged.

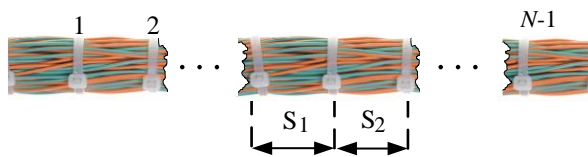


Fig. 1. Photo of the hand-assembled cable bundles.

Hand-assembled cable bundles change irregularly and randomly along the longitudinal dimension of the wiring harness. The randomness of wiring harness can be described by twisting degree β ($\beta \geq 0$). The more irregular the wiring harness is, the higher the twisting degree is. The twisting degree represents the number of segments divided per meter, which is obtained from experience. The number of segments N of the wiring harness is an integer related to twisting degree β , which satisfies the empirical formula:

$$N = \begin{cases} [\beta d] & \beta > \frac{1}{d} \\ 1 & \beta \leq \frac{1}{d} \end{cases}, \quad (1)$$

where $[\]$ is an integer symbol. The direction of the twisted wiring harness is arbitrary, and the number of twisted wires per segment is unknown (the wires in each segment are divided into twisted wires and untwisted wires).

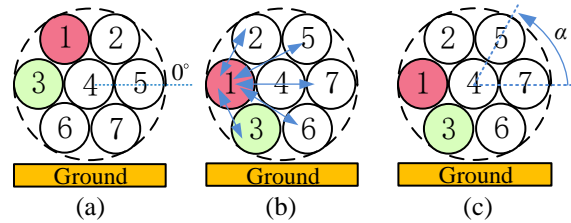


Fig. 2. Cross section of seven-core wiring harness: (a) reference, (b) position exchange, and (c) angle change.

According to the idea of the cascade method of the MTL, hand-assembled cable bundles can be segmented, and the wiring harness in the small segment can be regarded as a parallel MTL. For the convenience of the modeling process description, a seven-core wiring harness is used as an example. Along the axial direction, the wire position change may occur between the different segments, as shown in Fig. 2 (a) and Fig. 2 (b). In addition to the wire position change, the wiring harness may also have a rotation change of angle α ($\alpha \in [0, 360^\circ)$) as shown in Fig. 2 (a) and Fig. 2 (c). The effect of rotating a certain degree is similar to that of the wire position change. For example, the wiring harness in Fig. 2 (a) is rotated counterclockwise by 60° and is the same as the effect of Fig. 2 (b). However, only the rotation change cannot make the central wire (No. 4) in Fig. 2 participate in random exchange.

The schematic diagram of random harness modeling is shown in Fig. 3. Figure 3 (a) is a model schematic diagram of parallel MTL. Figure 3 (b) is a model schematic diagram considering only the random exchange of wires position, in which the geometric shapes of the cross section are unchanged relative to the reference ground. In this paper, if there is no special explanation, “random” refers to a random function that obeys uniform

distribution. Figure 3 (c) is a schematic diagram of a random harness model considering both the random rotation angle factor and the wires position exchange. Figure 3 (d) is a wire harness model diagram corresponding to Fig. 3 (c).

Obviously, if the positions of two wires can only be exchanged randomly at a time without considering the change of the rotation, any two cross sections can be converted to each other by $n-1$ exchange at most.

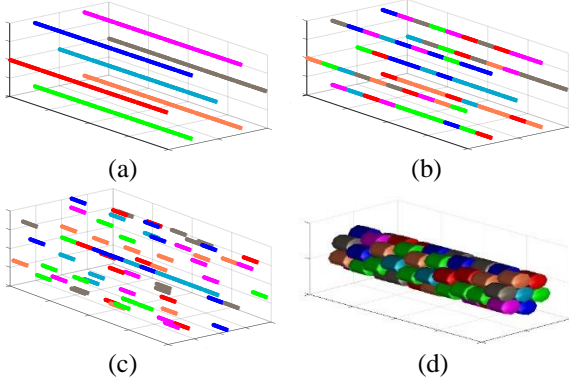


Fig. 3. Model of seven-core wiring harness: (a) parallel, (b) random exchange of wires position, (c) random rotation based on the exchange of wires position, and (d) hand-assembled cable bundles.

III. CROSSTALK ANALYSIS OF HAND-ASSEMBLED CABLE BUNDLES

A. The p.u.l. RLCG parameter matrix considering the random exchange of wires position

For ease of study, consider only the changes in Fig. 3 (a) to Fig. 3 (b) in this part. The equivalent circuit of the p.u.l. MTLs is shown in Fig. 4, where dz is expressed as an infinitely short transmission line. The p.u.l. resistances of the circuit are represented by the entries r_i and r_j . The p.u.l. self-inductances and mutual inductances of the circuit are denoted by the entries l_{ii} and l_{ij} . The p.u.l. self-capacitances and mutual capacitances of the circuit are expressed by the entries c_{ii} and c_{ij} . The p.u.l. conductances of the circuit are described by the entries g_{ii} and g_{ij} . The resistance R , the inductance L , the capacitance C and the conductance G parameter matrix of the n -core wiring harness on the return plane are all $n \times n$ order matrices [3]. Specifically expressed as:

$$X = \begin{bmatrix} x_{11} & x_{12} & \cdots & x_{1i} & \cdots & x_{1j} & \cdots & x_{1n} \\ x_{21} & x_{22} & \cdots & x_{2i} & \cdots & x_{2j} & \cdots & x_{2n} \\ \vdots & \vdots & \ddots & \vdots & \ddots & \vdots & \ddots & \vdots \\ x_{i1} & x_{i2} & \cdots & x_{ii} & \cdots & x_{ij} & \cdots & x_{in} \\ \vdots & \vdots & \ddots & \vdots & \ddots & \vdots & \ddots & \vdots \\ x_{j1} & x_{j2} & \cdots & x_{ji} & \cdots & x_{jj} & \cdots & x_{jn} \\ \vdots & \vdots & \ddots & \vdots & \ddots & \vdots & \ddots & \vdots \\ x_{n1} & x_{n2} & \cdots & x_{ni} & \cdots & x_{nj} & \cdots & x_{nn} \end{bmatrix}, \quad (2)$$

where X stands for the R , L , C , and G parameter matrices, and the parameter matrix X is a symmetric matrix. x represents the value of resistance r , the inductance l , the capacitance c and the conductance g corresponding to different parameter matrices.

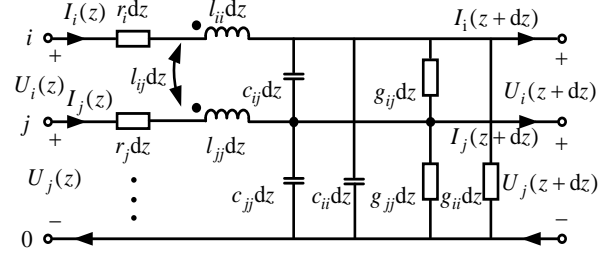


Fig. 4. The equivalent circuit of per unit length MTLs.

The transmission line equations are:

$$\frac{\partial}{\partial z} V(z,t) = -R(z)I(z,t) - L(z) \frac{\partial}{\partial t} I(z,t), \quad (3)$$

$$\frac{\partial}{\partial z} I(z,t) = -G(z)V(z,t) - C(z) \frac{\partial}{\partial t} V(z,t), \quad (4)$$

where $V(z,t)$ and $I(z,t)$ are voltages and currents at different locations and at different times on the MTLs [3]. The $R(z)$, $L(z)$, $C(z)$, and $G(z)$ parameter matrices are variables with respect to the position z of the MTLs, and the MTLs at different positions of the wiring harness may have different parameter matrices. According to the model of hand-assembled cable bundles in the previous section, it can be known that the position of the wires in the cross section of the segmented wiring harness has changed relative to the reference cross section.

Assume that only two wires have exchanged positions which are the i -th and j -th wires, respectively, and the corresponding parameter matrix after the exchange can be expressed as:

$$X' = \begin{bmatrix} x_{11} & x_{12} & \cdots & x_{1j} & \cdots & x_{1i} & \cdots & x_{1n} \\ x_{21} & x_{22} & \cdots & x_{2j} & \cdots & x_{2i} & \cdots & x_{2n} \\ \vdots & \vdots & \ddots & \vdots & \ddots & \vdots & \ddots & \vdots \\ x_{j1} & x_{j2} & \cdots & x_{jj} & \cdots & x_{ji} & \cdots & x_{jn} \\ \vdots & \vdots & \ddots & \vdots & \ddots & \vdots & \ddots & \vdots \\ x_{i1} & x_{i2} & \cdots & x_{ij} & \cdots & x_{ii} & \cdots & x_{in} \\ \vdots & \vdots & \ddots & \vdots & \ddots & \vdots & \ddots & \vdots \\ x_{n1} & x_{n2} & \cdots & x_{nj} & \cdots & x_{ni} & \cdots & x_{nn} \end{bmatrix}. \quad (5)$$

It can be seen from (2) and (5) that the row and column parameters irrelevant to i and j in the two parameter matrices remain unchanged. The parameter matrix in (5) can be obtained by exchanging the parameter matrix in (2) between the i -th row and the j -th row and between the i -th column and the j -th column.

The elementary matrix P_{ij} is defined as the matrix after the exchange of the i -th and the j -th row (or the i -th and the j -th column) of the identity matrix:

$$P_{ij} = \begin{bmatrix} 1 & 0 & \dots & 0 & \dots & 0 & \dots & 0 \\ 0 & 1 & \dots & 0 & \dots & 0 & \dots & 0 \\ \vdots & \vdots & \ddots & \vdots & \vdots & \vdots & \vdots & \vdots \\ 0 & 0 & \dots & 0 & \dots & 1 & \dots & 0 \\ \vdots & \vdots \\ 0 & 0 & \dots & 1 & \dots & 0 & \dots & 0 \\ \vdots & \vdots & \vdots & \vdots & \vdots & \vdots & \ddots & \vdots \\ 0 & 0 & \dots & 0 & \dots & 0 & \dots & 1 \end{bmatrix}. \quad (6)$$

The relationship between X and X' can be expressed as:

$$X' = P_{ij} X P_{ij}. \quad (7)$$

When there are more than two wires exchange positions in the small segment, the parameter matrix after the exchange can be expressed as:

$$X' = P_k \dots P_1 X P_1 \dots P_k, \quad (8)$$

where $P_i (i=1,2,\dots,k)$ is an elementary matrix, k is the number of wire exchanges, $1 \leq k \leq n-1$.

The p.u.l. RLCG parameter matrix of any small segment in Fig. 3 (b) can be obtained by (8).

B. The p.u.l. RLCG parameter matrix considering the change of rotation angle

The analysis of the previous part only considers the wire position exchange in the small segment, without considering the rotation angle of the small segment to the ground. Since the hand-assembled cable bundles are the random harness, the position of the wires and the rotation angle of the small segments are both random. Different rotation angles correspond to different RLCG parameter matrices. It is difficult to obtain a parameter matrix of an arbitrary rotation angle by a conventional method. Any determined rotation angle of the small segment has its unique corresponding parameter matrix. There is a nonlinear mapping relationship between the rotation angle and the parameter matrix. Therefore, an algorithm with strong nonlinear mapping ability, BP neural network, is introduced in this paper. The specific mapping relationship is shown in Fig. 5.

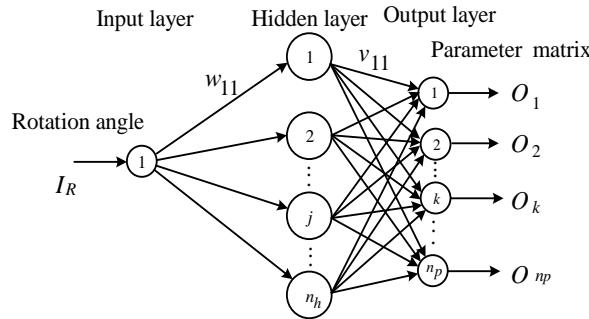


Fig. 5. Mapping topology of rotation degree and parametric matrix based on BP neural network.

In Fig. 5, the input parameter is the degree of rotation I_R , and the number of corresponding neurons is one. The output parameter is the RLCG parameter matrix, which is represented by the array $O_P=[O_1, O_2, \dots, O_{n_p}]$, where n_p is the number of corresponding neurons. Its value is equal to the number of elements of the RLCG parameter matrix. According to the actual cross section, samples of the parameter matrix under different rotation degrees are collected and used to train the BP neural network. The BP neural network structure used in Fig. 5 belongs to the small to medium neural network, so one hidden layer can meet the requirements. The number of neurons in the hidden layer n_h is an empirical range value determined by the number of neurons in the input layer and the output layer, specifically:

$$n_h = \sqrt{1+n_p} + n_c, \quad (9)$$

where n_c stands for a constant of the interval $[0, 10]$, and the specific value depends on the specific situation.

The sigmoid function $f_1(x)$ is used for input layer to hidden layer, and the linear function $f_2(x)$ is used for hidden layer to output layer. Respectively,

$$f_1(x) = \frac{1}{1+e^{-x}}, \quad (10)$$

$$f_2(x) = x. \quad (11)$$

After the signal propagates forward through the input layer, hidden layer and output layer of BP neural network, the p.u.l. RLCG parameter matrix output value O_k of the k -th output layer is:

$$O_k = \sum_{j=1}^{n_h} \frac{v_{jk}}{\exp(-(w_{1j} I_R + \theta_j)) + 1} + b_k, \quad (12)$$

where w_{1j} denotes the weight between the input layer and the j -th hidden layer. The threshold of the j -th hidden layer is represented by θ_j . The weight between the j -th hidden layer and the k -th output layer is denoted by v_{jk} . The threshold of the k -th output layer is indicated by b_k .

The training sample data group is m . The iteration is stopped when the mean square error (MSE) between the output value and the target RLCG parameter matrix value y is less than the error precision E or the training times is not less than the max-epoch. Then the BP neural network outputs the weights and thresholds of each layer. Otherwise, training will continue. The error precision E can be expressed as:

$$E = \frac{1}{2m} \sum_{i=1}^m \sum_{j=1}^{n_p} (O_{ij} - y_{ij})^2, \quad (13)$$

where O_{ij} stands for the value of the RLCG parameter matrix obtained by the j -th neuron of the output layer after the i -th training sample passes through the BP neural network. The sample standard value is represented by y_{ij} .

The training process is the adjustment process of the weights and thresholds. The weights of the two layers are similar to the threshold adjustment method. The weights between the hidden and output layer adjustment are illustrated as an example. The Levenberg - Marquardt (L-M) algorithm is used to adjust the values:

$$w_{k+1} = w_k + \Delta w_k, \quad (14)$$

$$\Delta w_k = -[J^T(w_k)J(w_k) + \mu I]^{-1} J^T(w_k) * e, \quad (15)$$

where w_k and w_{k+1} are the weights before and after the adjustment of each layer, respectively. And where J denotes the Jacobi matrix of the error e with respect to the weight w , μ is the scalar factor, and I stands for the identity matrix. The L-M algorithm controls the speed of the iteration by changing the value of μ . The error e is the MSE of each layer corresponding to each training sample:

$$e = \frac{1}{2} \sum_{k=1}^{n_p} (O_k - y_k)^2, \quad (16)$$

where O_k represents the network output value of the hidden layer or the output layer and where y_k is the sample standard value. Through the analysis of this part, we obtain the p.u.l. RLCG parameter matrix considering the rotation angle of the small segment to the ground.

C. Crosstalk analysis

The transmission line equations (3) and (4) are processed by the Wendroff differential format to obtain the FDTD method expression of crosstalk [24]. The FDTD method divides the transmission line into a large number of small segments, and the number of small segments NDZ divided by the FDTD method is far more than the wiring harness segments N . Therefore, the crosstalk of the hand-assembled cable bundles can be calculated by the FDTD method in this paper.

The flow chart of crosstalk prediction for random wiring harness is shown in Fig. 6. It can be seen from the flow chart that the crosstalk solution of the segmented wiring harness can be divided into two parts, which are the extraction of the parameter matrix of each segment and the crosstalk solution using the FDTD method, respectively. In the process of extracting the parameter matrix for each segment, the RLCG parameter matrix samples with different rotation degrees are extracted by using the ANSYS Q3D software based on the finite element method (FEM) after selecting a reference cross section. The BP neural network that can map any rotation degree is obtained by training samples. Remarkably, the rotation degree of each segment to the ground is generated randomly in the interval $[0, 360^\circ]$, and the corresponding parameter matrix can be quickly solved by combining the trained BP neural network. In wire exchange, the number of exchanges is generated randomly in the interval $[1, n-1]$, which corresponds to the number of elementary transformations of the p.u.l. RLCG parameter matrix. The number of two wires

exchanged each time is a random number on the interval $[1, n]$, which determines the elementary matrix of each transformation. According to the basic idea of the Monte Carlo method, the numerical characteristics of random variables can be used as a reference for the solution of the problem.

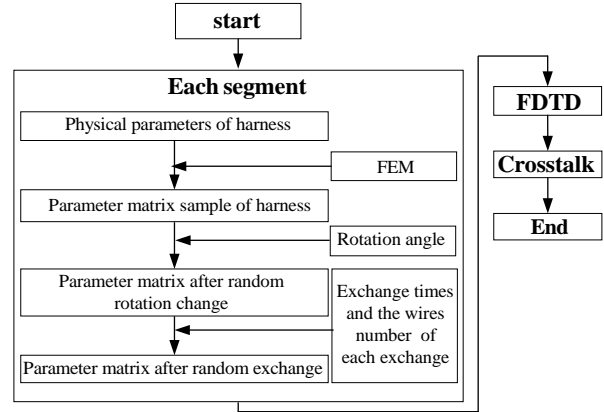


Fig. 6. Flow chart of random wiring harness crosstalk prediction.

IV. VERIFICATION AND ANALYSIS

In this paper, the seven-core hand-assembled cable bundles are used as an example to verify and analyze the new method. The single wire radius in the wiring harness is 0.4 mm and consists of 25 strands of thin copper wire. The insulating material of the wire is the polyvinyl chloride (PVC) with the relative permittivity of 2.7 and the thickness is 0.6 mm . The wire length is 3 m , and each end is terminated with a 50Ω resistor. The details are shown in Table 1.

Table 1: Basic parameter of wiring harness

Name	Parameter
Single conductor radius	0.4 mm
Insulation thickness	0.6 mm
Insulation materials	PVC
Length	3 m
Terminated impedance	50Ω

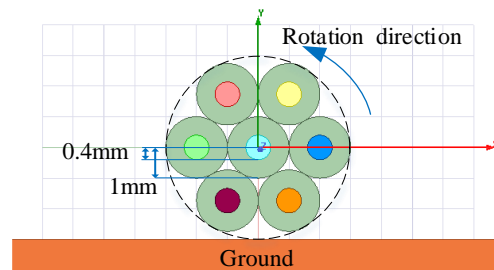


Fig. 7. The cross section and return plane of the seven-core wiring harness.

The cross section showed in Fig. 7 is taken as the reference cross section. The effect of the R and G parameters is ignored because the termination resistance value is much larger than the wire resistance. The inductance L and capacitance C parameter matrices of the reference cross section are:

$$L = \begin{bmatrix} 614.66 & 291.26 & 252.65 & 248.53 & 167.52 & 107.35 & 91.27 \\ 291.26 & 614.62 & 167.56 & 248.51 & 252.51 & 91.34 & 107.24 \\ 252.65 & 167.56 & 533.68 & 211.02 & 116.49 & 147.85 & 81.37 \\ 248.53 & 248.51 & 211.02 & 519.03 & 210.94 & 144.18 & 144.06 \\ 167.52 & 252.51 & 116.49 & 210.94 & 533.51 & 81.40 & 147.67 \\ 107.35 & 91.34 & 147.85 & 144.18 & 81.40 & 378.47 & 92.35 \\ 91.27 & 107.24 & 81.37 & 144.06 & 147.67 & 92.35 & 378.14 \end{bmatrix} \text{ nH/m}, \quad (17)$$

$$C = \begin{bmatrix} 64.61 & -21.39 & -21.00 & -15.45 & -1.024 & -0.67 & -0.12 \\ -21.39 & 64.61 & -1.03 & -15.45 & -20.99 & -0.12 & -0.67 \\ -21.00 & -1.03 & 66.10 & -15.41 & -0.19 & -18.80 & -0.51 \\ -15.45 & -15.45 & -15.41 & 93.00 & -15.41 & -15.17 & -15.18 \\ -1.024 & -20.99 & -0.19 & -15.41 & 66.082 & -0.51 & -18.80 \\ -0.67 & -0.12 & -18.80 & -15.17 & -0.51 & 82.01 & -15.41 \\ -0.12 & -0.67 & -0.51 & -15.18 & -18.80 & -15.41 & 82.00 \end{bmatrix} \text{ pF/m}. \quad (18)$$

The parameter matrix of different rotation angles is sampled relative to the reference cross section, and the sampling rotation direction is shown in Fig. 7. All cross sections can be obtained by considering the rotation angle in the range of $[0, 60^\circ)$ and the random exchange of wires since the model discussed is axisymmetric. Samples were collected every 10° for a total of 12 groups.

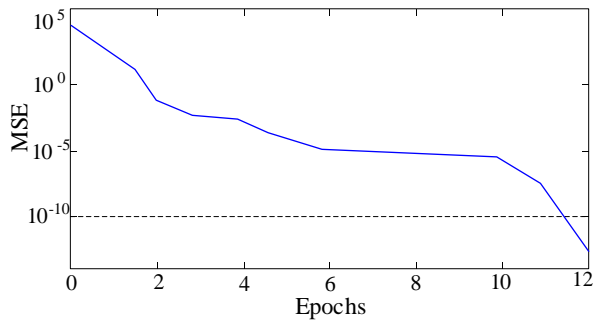


Fig. 8. Iteration number and MSE.

The relationship between the number of iterations and the training MSE of BP neural network is shown in Fig. 8. The training network satisfies the target MSE ($E=10^{-10}$) when the number of iterations is 12.

In order to verify the correctness and effectiveness of the proposed method, a simple crosstalk test platform is built shown in Fig. 9. The corresponding experimental schematic diagram is shown in Fig. 10. The whole wiring harness is placed on the return plane of the same length, and the width of the return plane is much larger than the distance of the harness from the return plane. The material of the return plane is copper. The Agilent 87511A vector network analyzer (VNA) is used as a measuring device.

The crosstalk comparison results of the seven-core hand-assembled cable bundles with the twisting degree

$\beta=6$ and $\beta=2$ are shown in Fig. 11 (a) and Fig. 11 (b), respectively. The green solid line represents the result of the new method. The blue solid line stands for the result of the experiment. The red dashed line is the outer envelope of the green line. And the black dashed line is the outer envelope of the result of the probability method [25]. It can be observed in Fig. 11 that the experimental results and the method presented in this paper have high consistency. The experimental results are almost within the upper envelope of the results of the proposed method, which means that the proposed method can predict the “worst case” crosstalk of the harness. By comparison, the higher the twisting degree, the more concentrated the crosstalk, and the crosstalk of the low frequency band is more concentrated than the high frequency band. It can be understood that the higher the twisting degree of the wiring harness, the more the crosstalk tends to “average”, so the more the crosstalk is concentrated. The more concentrated the curves, the smaller the distance between the upper and lower envelopes of the predicted value.

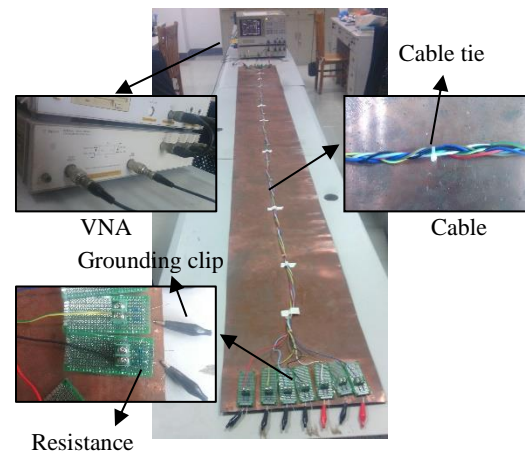


Fig. 9. Crosstalk measurement experimental platform.

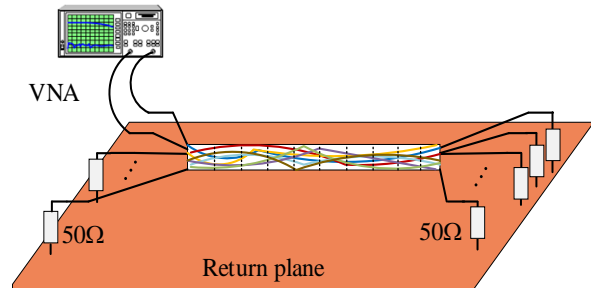


Fig. 10. Schematic diagram of experiment.

In the frequency band of 0.1 MHz - 3 MHz, both the new method and the probability method can predict the “worst case” crosstalk of the harness, but the distance between the lower envelope and upper envelope of the

new method is obviously smaller than that of the probability method. The accuracy of the new method is higher than that of the probability method. In the frequency band of 3 MHz - 40 MHz, the accuracy of the new method is higher than that of the probability method. The lower envelope of the probability method at some frequency points is even larger than the maximum of the experimental results in Fig. 11 (b). Moreover, the prediction range of the probability method in the frequency band of 10 MHz - 25 MHz is too large and has little practical significance. In the frequency band of 40 MHz-100 MHz, the accuracy of the new method and the probability method is not as good as that of the low frequency band, but the trend of the new method is closer to the experimental results. The trend predicted by probability method is not consistent with the experimental results and the range of predicted values is too large.

In [17], it mainly aims at the frequency band less than 10^7 Hz. Compared with [17], the crosstalk frequency band predicted by the new method is wider.

However, it can be clearly seen that at some points of high frequency, the lower envelope and the upper envelope solved by the new method or the probability method are not completely consistent with the experimental test results. The possible reason is that the high frequency characteristics of the components and devices used in the experiment are not completely ideal.

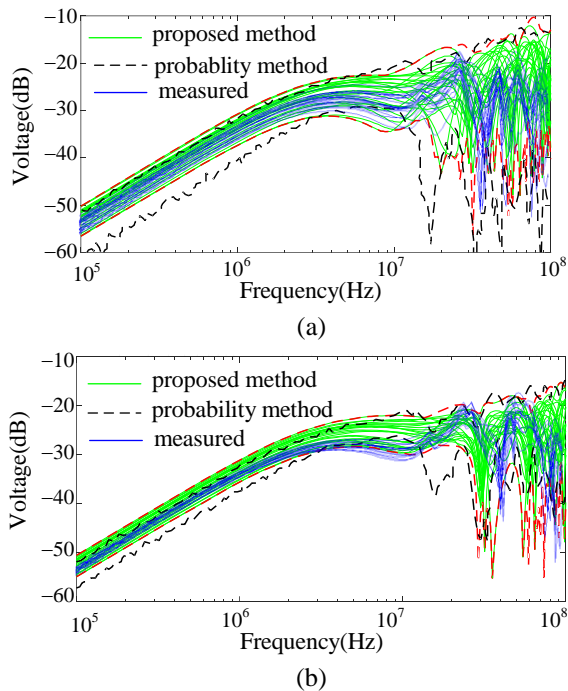


Fig. 11. Comparison of seven-core hand-assembled cable bundles crosstalk solved by different methods: (a) $\beta = 2$ and (b) $\beta = 6$.

V. CONCLUSION

The crosstalk of hand-assembled cable bundles based on the FDTD method is studied in this paper. The comparison between experiment and simulation shows that after 12 iterations, BP neural network can reflect the mapping of the rotation degree and the p.u.l. RLCG parameter matrix. The proposed method has better prediction accuracy than probability method for the crosstalk of random wiring harness. The crosstalk of wiring harness is widely distributed in high frequency band and relatively concentrated in low frequency band. The higher the twisting degree of the wiring harness, the more concentrated the crosstalk in the whole frequency band.

ACKNOWLEDGMENT

The work was supported by National Natural Science Foundation of China under Grant No.51475246, National Natural Science Foundation of Jiangsu Province under Grant No.BK20161019, and Aviation Science Foundation under Grant No.20172552017.

REFERENCES

- [1] S. Chabane, P. Besnier, and M. Klingler, "A modified enhanced transmission line theory applied to multiconductor transmission lines," *IEEE Trans. on Electromagn. Compat.*, vol. 59, no. 2, pp. 518-528, Apr. 2017.
- [2] Y. Wang, Y. S. Cao, D. Liu, R. W. Kautz, N. Altunyurt, and J. Fan, "A generalized multiple-scattering method for modeling a cable harness with ground connections to a nearby metal surface," *IEEE Trans. Electromagn. Compat.*, vol. 61, no. 1, pp. 261-270, Feb. 2019.
- [3] C. R. Paul, *Analysis of Multiconductor Transmission Lines*. Wiley, New York, 1994.
- [4] S. Shiran, B. Reiser, and H. Cory, "A probabilistic method for the evaluation of coupling between transmission lines," *IEEE Trans. Electromagn. Compat.*, vol. 35, no. 3, pp. 387-393, Aug. 1993.
- [5] C. R. Paul, "Sensitivity of crosstalk to variations in wire position in cable bundles," *1987 IEEE International Symposium Electromagnetic Compatibility*, Atlanta, GA, pp. 1-5, Aug. 1987.
- [6] Z. Fei, Y. Huang, J. Zhou, and Q. Xu, "Uncertainty quantification of crosstalk using stochastic reduced order models," *IEEE Trans. Electromagn. Compat.*, vol. 59, no. 1, pp. 228-239, Feb. 2017.
- [7] G. Spadacini, F. Grassi, and S. A. Pignari, "Field-to-wire coupling model for the common mode in random bundles of twisted-wire pairs," *IEEE Trans. Electromagn. Compat.*, vol. 57, no. 5, pp. 1246-1254, Oct. 2015.
- [8] S. A. Pignari, G. Spadacini, and F. Grassi, "Modeling field-to-wire coupling in random

- bundles of wires,” *IEEE Electromagnetic Compatibility Magazine*, vol. 6, no. 3, pp. 85-90, Nov. 2017.
- [9] M. Gonser, C. Keller, J. Hansen, and R. Weigel, “Advanced simulations of automotive EMC measurement setups using stochastic cable bundle models,” *2010 Asia-Pacific International Symposium on Electromagnetic Compatibility*, Beijing, China, pp. 590-593, Apr. 2010.
- [10] A. Ciccolella and F. G. Canavero, “Stochastic prediction of wire coupling interference,” *Proceedings of International Symposium Electromagnetic Compatibility.*, Atlanta, GA, pp. 51-56, Aug. 1995.
- [11] P. Manfredi, D. De Zutter, and D. V. Ginste, “Analysis of coupled exponential microstrip lines by means of a multi-step perturbation technique,” *IEEE 20th Workshop on Signal and Power Integrity (SPI)*, Turin, Italy, pp. 1-4, May 2016.
- [12] D. Bellan and S. A. Pignari, “Statistical superposition of crosstalk effects in cable bundles,” *China Communications*, vol. 10, no. 11, pp. 119-128, Nov. 2013.
- [13] J. C. Pincetti and P. L. E. Uslenghi, “Incident field excitation of random cables,” *Radio Science*, vol. 42, no. 06, pp. 1-10, Dec. 2007.
- [14] D. Bellan and S. A. Pignari, “Efficient estimation of crosstalk statistics in random wire bundles with lacing cords,” *IEEE Trans. Electromagn. Compat.*, vol. 53, no. 1, pp. 209-218, Feb. 2011.
- [15] S. Sun, G. Liu, J. L. Drewniak, and D. J. Pommerenke, “Hand-assembled cable bundle modeling for crosstalk and common-mode radiation prediction,” *IEEE Trans. Electromagn. Compat.*, vol. 49, no. 3, pp. 708-718, Aug. 2007.
- [16] M. Wu, D. Beetner, T. Hubing, Haixin Ke, and S. Sun, “Estimation of the statistical variation of crosstalk in wiring harnesses,” *2008 IEEE International Symposium on Electromagnetic Compatibility*, Detroit, MI, pp. 1-7, Aug. 2008.
- [17] M. Wu, D. G. Beetner, T. H. Hubing, H. Ke, and S. Sun, “Statistical prediction of “Reasonable Worst-Case” crosstalk in cable bundles,” *IEEE Trans. Electromagn. Compat.*, vol. 51, no. 3, pp. 842-851, Aug. 2009.
- [18] S. Salio, F. Canavero, D. Lecointe, and W. Tabbara, “Crosstalk prediction on wire bundles by Kriging approach,” *IEEE International Symposium on Electromagnetic Compatibility*, Washington, DC, vol. 1, pp. 197-202, Aug. 2000.
- [19] A. Tatematsu, F. Rachidi, and M. Rubinstein, “A technique for calculating voltages induced on twisted-wire pairs using the FDTD method,” *IEEE Trans. Electromagn. Compat.*, vol. 59, no. 1, pp. 301-304, Feb. 2017.
- [20] V. R. Kumar, B. K. Kaushik, and A. Patnaik, “An accurate FDTD model for crosstalk analysis of CMOS-Gate-Driven coupled RLC interconnects,” *IEEE Trans. Electromagn. Compat.*, vol. 56, no. 5, pp. 1185-1193, Oct. 2014.
- [21] T. Rashid, *Make Your Own Neural Network*, Charleston. Create Space Independent Publishing Platform, Charleston, 2016.
- [22] M. Hassoun, *Fundamentals of Artificial Neural Networks*, Bradford Book, Cambridge, 2003.
- [23] F. Dai, G. Bao, and D. Su, “Crosstalk prediction in non-uniform cable bundles based on neural network,” *Proceedings of the 9th International Symposium on Antennas, Propagation and EM Theory*, Guangzhou, China, pp. 1043-1046, Nov. 2010.
- [24] L. Brančik and N. Al-Zubaidi R-Smith, “Comparative simulations of hybrid systems with nonuniform MTLs via Wendroff and NILT based techniques,” *2016 Progress in Electromagnetic Research Symposium (PIERS)*, Shanghai, China, pp. 4067-4072, Aug. 2016.
- [25] Z. Zhang, S. Wang, and L. Zhao, “Prediction of crosstalk probability distribution in cable bundles,” *Transactions of China Electrotechnical Society*, vol. 32, no. 7, pp. 203-214, Apr. 2017.



Chengpan Yang was born in Sichuan Province, China. He received the B.S. degree in School of Automation and Information Engineering from Sichuan University of Science and Engineering, Zigong, China, in 2017. He is currently working toward the Master’s degree in electrical engineering at Nanjing Normal University, Nanjing, China. His major research interests include new technology of electrical engineering.



Wei Yan Doctor & Assoc. Professor from Nanjing Normal University. He obtained the Physics and Electronics Ph.D and Electrical Engineering M.S. from Nanjing Normal University in 2014 and 2011. He is the Senior Member of China Electrical Technology Association and the evaluation expert of the Electromagnetic Compatibility Calibration Specification of China.



Yang Zhao received his B.E., M.E., and Ph.D. degree all in Power Electronic Technology from Nanjing University of Aeronautics and Astronautics, Nanjing, China, in 1989 and 1992, and 1995, respectively. He is currently the Professor with Nanjing Normal University. His research interests are in the areas of Electromagnetic Compatibility, Power Electronics and Automotive Electronics.



Shishan Wang received the Ph.D. degree from Xi'an Jiaotong University, Xi'an, China, in 2003. Since 2004, he has been an Associate Professor with the College of Automation Engineering Nanjing University of Aeronautics and Astronautics, Nanjing, China. His main research interests include electromagnetic compatibility in power electronics system and simulation of multiphysics fields for electrical equipment.



Qiangqiang Liu was born in Anhui Province, China. He received the B.S degree in school of Electrical Engineering and Automation from Anhui University of Science and Technology, Huainan, China, in 2018. He is currently working toward the Master's degree in Electrical Engineering at Nanjing Normal University, Nanjing, China. His major research interests include new technology of electrical engineering.